International Journal of Biochemistry and Cell Biology 112 (2019) 134–140

Contents lists available at ScienceDirect

International Journal of Biochemistry and Cell Biology

journal homepage: www.elsevier.com/locate/biocel

Evaluation of differentially expressed microRNAs in vitrified oocytes by next generation sequencing

Jun Li*, Xuemei Yang, Fang Liu, Yaman Song, Yuanke Liu

Department of Reproductive Medicine, The First Hospital of Hebei Medical University, Shijiazhuang, Hebei, 050031, PR China

ARTICLE INFO

Keywords:
microRNAs
Oocyte vitrification
Sequencing
PTEN

ABSTRACT

MicroRNAs (miRNAs) play crucial roles in gametogenesis and embryo development. The present study was undertaken to identify differentially expressed miRNAs and explore their functions in oocyte vitrification. Small RNA sequencing data revealed that 22 miRNAs were differentially expressed in vitrified oocytes compared with that of the fresh counterparts. The potential target genes for the differentially expressed miRNAs were enriched in "anatomical development" in biological process, "cell" in cellular components, and "protein binding" in molecular functions by gene ontology annotation analysis. In addition, "endometrial cancer" and "metabolic pathway" were the two pathways enriched in KEGG with the lowest p-value and highest count number genes, respectively. RT-qPCR data showed that miR-134-5p, miR-210-5p, and miR-21-3p were significantly up-regulated ($P < 0.01$), whereas miR-465c-5p was dramatically down-regulated ($P < 0.01$) in vitrified oocytes, which were consistent with that of the sequencing result. Moreover, the expression of potential target PTEN was significantly reduced both at transcriptional ($P < 0.01$) and post-transcriptional level ($P < 0.01$) in vitrified oocytes. The expression pattern of PTEN was negatively correlated with that of miR-21-3p. Dual-luciferase reporter assay further demonstrated that miR-21-3p could down-regulate PTEN by targeting its 3′UTR. In conclusion, our results demonstrated that specific miRNAs were differentially expressed in warmed oocytes, and decreased expression of PTEN was involved in response to vitrification stress.

1. Introduction

Oocyte vitrification provides great opportunity for female fertility preservation and has extensive applications in assisted reproductive medicine (Cil and Seli, 2013). Although pronounced achievements have been made in recent years (Practice Committees of American Society for Reproductive and Society for Assisted Reproductive, 2013; Rienzi et al., 2017), wide application of the technique has been limited by the decreased developmental potential of thawed oocytes (Goldman et al., 2013; Braga et al., 2016; Succu et al., 2018).

MicroRNAs (miRNAs), a subset of non-coding RNA class, have emerged as pivotal regulators in gene expression (Lim et al., 2005). Previously, significant shifts in miRNA expression profile were found in warmed blastocysts (Zhao et al., 2015) and sperm (Capra et al., 2017). It was also discovered that suppression of miR-762 was beneficial for vitrified oocytes' survival and developmental capacity (Wang et al., 2018b). Systematic investigation on the dynamic alterations of miRNAs after oocyte vitrification has not yet been conducted. Study revealed that miR-21 was distinctly increased in porcine MII oocytes compared with that of the GV ones (Song et al., 2016). And significantly increased miR-21 was detected at the end of *in vitro* maturation of bovine oocytes, although pre-miR-21 transcript was not statistically changed between immature and *in vitro* matured oocytes (Tscherner et al., 2018). MiR-21-3p along with miR-21-5p originates from the same precursor, pre-miR-21. Up-regulated miR-21-5p while down-regulated miR-21-3p was found in cumulus cells from poor responders (Karakaya et al., 2015). By far, the function of miR-21-3p in vitrified oocytes remains unknown.

Therefore, the present study was aimed to determine miRNAs expression profiles in fresh and vitrified oocytes by small RNA sequencing method, and RT-qPCR was applied to validate the sequencing results. Finally, the target gene for miR-21-3p was identified, with the purpose to explore the biological role of miRNAs played in oocyte vitrification.

2. Material and methods

2.1. Mouse experimental procedures

The experimental protocols and animal handling procedures were approved by the institutional ethical committee of the First Hospital of Hebei Medical University (2005).

* Corresponding author.
E-mail address: junliydyy@126.com (J. Li).

https://doi.org/10.1016/j.biocel.2019.05.006
Received 27 November 2018; Received in revised form 30 April 2019; Accepted 10 May 2019
Available online 17 May 2019
1357-2725/

Cumulus oocyte complexes (COCs) were obtained from oviduct ampullae of super ovulated Kunming mouse. After incubation with 80 IU/mL hyaluronidase (Vitrolife, Gothenburg, Sweden) for less than 1 min, denuded oocytes were obtained and transferred into G-IVF plus medium (Vitrolife, Gothenburg, Sweden). The denuded oocytes were randomly divided into control (fresh oocytes) and vitrified group. In the vitrified group, fresh oocytes were vitrified and thawed according to the manufacturer's instruction (Kitazato BioPharma Co., Shizuoka, Japan). After thawing, survived oocytes with intact zona pellucida and refractive ooplasm were transferred into G-IVF plus medium at 37 ℃ contained 6% CO_2 in humidified air. Fresh and vitrified oocytes were collected and immediately stored in liquid nitrogen for further use.

2.2. Small RNA sequencing

Total RNA was extracted from fresh and vitrified oocytes using miRNeasy kit (Qiagen, Hilden, Germany). Sequencing library was prepared according to TruSeq Small RNA Sample Prep Kits (Illumina, San Diego, USA) and six libraries were constructed with three duplicates in each sample. In brief, 3′ and 5′ adapters were sequentially connected to small RNA ends by T4 ligase 2, RT-PCR was then performed to create cDNA constructs. Following the purification of suitable cDNA fragments in the length of 140-160bp, the small RNA library was constructed and then sequenced by Illumina Hiseq 2000/2500 (Illumina, San Diego, USA), the read length was 50 nt with single end sequencing pattern.

2.3. Sequencing data analysis

A proprietary pipeline script, ACGT101-miR version 4.2 (LC Sciences, Houston, TX, USA) was used for sequencing data analysis. The raw RNA reads were processed to remove adapters, junk reads, and impurity sequences. High-quality reads ranged from 18nt-25nt were subjected to remove protein coding genes, rRNA, tRNA, snRNA, snoRNA, and repeat sequences. Finally, remaining clean reads were mapped to the latest miRBase version 22.0 (http://www.mirbase.org), using Bowtie aligner to identify known mouse (Mus musculus) miRNAs.

Differentially expressed miRNAs were determined by student's *t*-test with $P < 0.05$. The norm data were transformed to Z value and hierarchical clustering was performed in TIGR MultiExperiment Viewer 4.0 (MeV 4.0) software program (http://www.tm4.org/mev.html).

2.4. Gene function and pathway analysis

MiRanda and Targetscan were used to predict target genes for differentially expressed miRNAs. The enrichment of predicted genes in cellular component, molecular function, and biological process was analyzed through Gene Ontology (GO) database (http://www.geneontology.org). The pathway analysis of potentially differently expressed proteins was based on the Kyoto Encyclopedia of Genes and Genomes (KEGG) database (http://www.genome.jp/kegg/mapper.html) and significantly enriched pathways enriched in target gene candidates were identified using hyper geometric test where genes in the whole genome were set to be background.

2.5. RT-qPCR validation

Matured miRNAs from 200 oocytes were isolated by miRNeasy kit (Qiagen, Hilden, Germany) and reverse transcription was performed using the RevertAid First Strand cDNA Synthesis Kit (Thermo Fisher Scientific, Waltham, MA, USA). The primer sequences were presented in Table 1. Quantitative real-time PCR analysis was performed with the iQ™ SYBR® Green Supermix kit (Bio-Rad, Hercules, CA, USA) and the conditions were as follows: 95 ℃ for 2 min followed by 40 cycles of 95 ℃ for 10 s and 60 ℃ for 30 s. The expression levels of miRNAs were normalized to that of U6 as previously reported (Wang et al., 2017), and all experiments were repeated at least three times. The relative expression levels were calculated based on the $2^{-\Delta\Delta Ct}$ method.

2.6. Quantification of gene expression

Messenger RNA was extracted from 200 oocytes using miRNeasy kit (Qiagen, Hilden, Germany). After eliminated genomic DNA, the isolated mRNA was used as template for reverse transcription with Primescript RT reagent kit with gDNA Eraser (Takara, Tokyo, Japan). The PCR reaction was conducted using QuantiTect SYBR Green PCR reagents on a Light Cycler 480 (Roche, Basel, Switzerland) with the following program: 95 ℃ for 10 min, followed by 40 cycles of 95 ℃ 10 s, 60 ℃ 15 s, and 72 ℃ 20 s. All PCR reactions were conducted in triplicate. GAPDH was used as internal control as indicated previously (Gao et al., 2017) and fold changes were calculated with the $2^{-\Delta\Delta Ct}$ method. Primers used in the RT-qPCR are shown in Table 1.

2.7. Western blot

A pool of 1000 oocytes was lysed in RIPA lysis buffer (Beyotime, Shanghai, China). Proteins were separated by SDS-PAGE and electrophoetically transferred to PVDF membranes. After transfer, membranes were blocked in TBST containing 5% (w/v) non-fat powdered milk for 1 h, and then incubated with the primary antibodies against PTEN (1:1000, Proteintech Group, Wuhan, China) and GAPDH (1:3000, Atagenix, Wuhan, China) overnight at 4 ℃. After three washes with TBST 10 min each, then incubation with HRP-conjugated secondary antibody (1:5000, Proteintech Group, Wuhan, China), the protein bands were visualized by ChemiDoc™XRS + system (Bio-Rad, Hercules, CA, USA). Each protein expression level was normalized to that of GAPDH.

2.8. Luciferase activity assay

Two luciferase reporter plasmids (pGL-PTEN-646-652-wt and pGL-PTEN-5576-5582-wt) as well as the corresponding mutant forms (pGL-PTEN-646-652-mut and pGL-PTEN-5576-5582-mut) were constructed and inserted into the pGL-3 vector (Promega, Madison, WI, USA), for that two sequences in the 3′UTR of PTEN were predicted as the binding sites for miR-21-3p by TargetScan. The HEK293 T cell line was subjected to a co-transfection of pGL-PTEN-646-652-wt/ pGL-PTEN-646-652-mut with miR-21-3p mimic/miR-21-3p negative control, or pGL-PTEN-5576-5582-wt/ pGL-PTEN-5576-5582-mut with miR-21-3p mimic/miR-21-3p negative control. The cells were transfected with Lipofectamine 2000 (Invitrogen, Carlsbad, CA, USA) according to the manufacturer's instructions. Cells were collected after 48 h of transfection and luciferase activity was determined by dual-luciferase reporter assay system (Promega, Madison, WI, USA). The luciferase activity was calculated as the ratio of firefly luciferase to renilla luciferase activity in the corresponding well and further normalized against the pGL3 vector.

2.9. Statistical analysis

Data were analyzed by Student's *t* test using SPSS 21.0 statistical software (IBM, Chicago, IL, USA). Each experiment was repeated at least three times and $P < 0.05$ was considered statistically different.

3. Results

3.1. Differed miRNAs expression profile in vitrified oocytes

A number of 914,675 and 1,016,385 unique reads were acquired from the fresh and vitrified oocytes, respectively. The distribution of unique reads were mainly within the length of 21–24 nt (Fig.1), accounted for 66.72% and 63.29% of the total unique reads in oocytes from the control and vitrified groups, respectively. In total, 520

Table 1
Sequences of primers used in RT-qPCR.

Name of primer	Sequence (5′–3′)
Stem loop primers	
miR-21-3p	GTCGTATCCAGTGCGTGTCGTGGAGTCGGCAATTGCACTGGATACGACGACAGCCC
miR-465c-5p	GTCGTATCCAGTGCGTGTCGTGGAGTCGGCAATTGCACTGGATACGACCAGATCAG
miR-210-5p	GTCGTATCCAGTGCGTGTCGTGGAGTCGGCAATTGCACTGGATACGACCAGTGTGC
miR-134-5p	GTCGTATCCAGTGCGTGTCGTGGAGTCGGCAATTGCACTGGATACGACCCCCTCTG
U6	GAATTTGCGTGTCATCCTTG
qPCR primers	
miR-21-3p	F: TGCGCCAACAGCAGTCGATGAC
miR-465c-5p	F: TGCGCTATTTAGAATGGCGCAG
miR-210-5p	F: TGCGCAGCCACTGCCCACCCAG
miR-134-5p	F: TGCGCTGTGACTGGTTGACCCC
miR-universal-Reverse	R: CAGTGCGTGTCGTGGAGT
U6	F: GCTTCGGCAGCACATATACTAAAAT
	R: CGCTTCACGAATTTGCGTGTCAT
PTEN	F: CCCACCACAGCTAGAACTTATC
	R: CGTCCCTTTCCAGCTTTACA
GAPDH	F: TGTTTCCTCGTCCCGTAGA
	R: GATGGCAACAATCTCCACTTTG

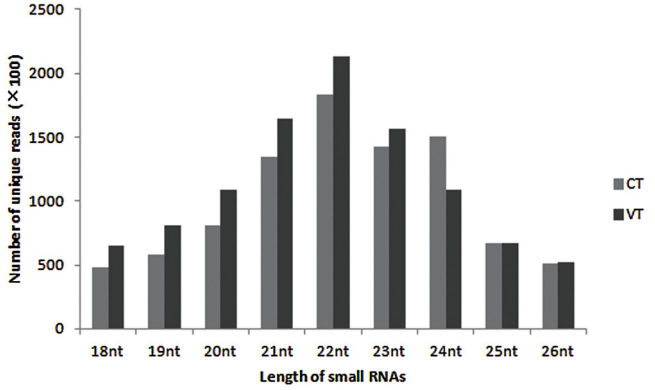

Fig. 1. Length distribution of small RNA sequences. CT, fresh oocytes; VT, vitrified oocytes.

Table 2
Summary of differentially expressed miRNAs.

miR_name	miR_seq	Fold change (VT/CT)	*P* value
miR-465c-5p	TATTTAGAATGGCGCTGATCTG	0.58	2.38E-03
miR-134-5p	TGTGACTGGTTGACCAGAGGGG	2.91	5.13E-03
miR-21-3p	CAACAGCAGTCGATGGGCTGTC	2.34	1.11E-02
miR-345-5p_L+1R-1	TGCTGACCCCTAGTCCAGTGCT	1.64	1.40E-02
miR-741-3p_R-1	TGAGAGATGCCATTCTATGTAG	0.70	1.54E-02
miR-132-5p_L-1R+1	ACCGTGGCTTTCGATTGTTACT	1.35	1.55E-02
miR-191-5p_R-1	CAACGGAATCCCAAAAGCAGCT	1.25	1.59E-02
miR-132-3p	TAACAGTCTACAGCCATGGTCG	1.46	1.88E-02
miR-181a-1-3p	ACCATCGACCGTTGATTGTACC	1.98	1.92E-02
miR-149-5p	TCTGGCTCCGTGTCTTCACTCCC	1.23	1.97E-02
miR-532-3p	CCTCCCACACCCAAGGCTTGCA	1.53	2.59E-02
miR-26a-5p_L+1	CTTCAAGTAATCCAGGATAGGCT	0.54	2.67E-02
miR-210-5p	AGCCACTGCCCACCGCACACTG	3.57	2.75E-02
miR-296-3p	GAGGGTTGGGTGGAGGCTCTCC	2.03	3.11E-02
miR-27b-5p_R+1	AGAGCTTAGCTGATTGGTGAACA	inf	3.50E-02
miR-190a-5p_R+1	TGATATGTTTGATATATTAGGTT	0.63	3.73E-02
miR-3068-5p	TTGGAGTTCATGCAAGTTCTAACC	0.32	4.03E-02
miR-664-3p_R+1	TATTCATTTACTCCCCAGCCTAC	0.53	4.08E-02
miR-324-3p_L-2R+3	ACTGCCCCAGGTGCTGCTGGT	1.68	4.30E-02
miR-465a-5p	TATTTAGAATGGCACTGATGTGA	0.67	4.31E-02
miR-433-3p	ATCATGATGGGCTCCTCGGTGT	1.62	4.63E-02
miR-99b-5p	CACCCGTAGAACCGACCTTGCG	1.32	4.88E-02

miRNAs were identified in oocytes, and among them, 22 miRNAs were significantly different expressed in vitrified oocytes compared with that of the fresh counterparts ($P < 0.05$, Table 2). Unsupervised hierarchical clustering analysis was performed to elucidate the distinctions between different samples and their biological relevance. Two groups, fresh and vitrified oocytes, were divided according to the miRNAs expression profiles (Fig.2).

3.2. Target enrichment analysis for differentially expressed miRNAs

GO enrichment found that the potential targets were mainly enriched in “anatomical development” in biological process, “cell” in cellular components, and “protein binding” in molecular functions (Fig.3). To identify the biological pathway influenced by vitrification, predicted genes of the differentially expressed miRNAs were assigned to KEGG pathways with enrichment statistics (Fig.4). The top five enrichment pathways sorted by p-value were “endometrial cancer”, “insulin signaling pathway”, “acute myeloid leukemia”, “metabolic pathways”, and “pathways in cancer”. The pathways with the highest gene count numbers was sorted as “metabolic pathway”.

3.3. RT-qPCR validated sequencing data

Four dramatically differentially expressed miRNAs (miR-21-3p, miR-465c-5p, miR-210-5p, and miR-134-5p) were selected to be quantified by RT-qPCR. As shown in Fig.5, the expression level of miR-465c-5p was significantly down-regulated ($P < 0.01$) while the expression levels of miR-21-3p, miR-210-5p, and miR-134-5p were significantly elevated in the vitrified oocytes compared with that of the fresh group ($P < 0.01$), which were consistent with the sequencing data.

3.4. Potential functional analysis of miR-21-3p

Dramatically decreased PTEN expression was assessed in vitrified oocytes in comparison with that of the fresh ones both at transcriptional (Fig. 6A) and post-transcriptional level ($P < 0.01$) (Fig. 6B). Moreover, markedly decreased luciferase activities in both plasmids with predicted binding sites of PTEN 3′UTR were observed when co-transfected with miR-21-3p mimic ($P < 0.01$) (Fig. 7).

4. Discussion

In consistency with the defined length of miRNAs (Ambros, 2004; Bartel, 2004), the length distribution of sequenced miRNAs in the study

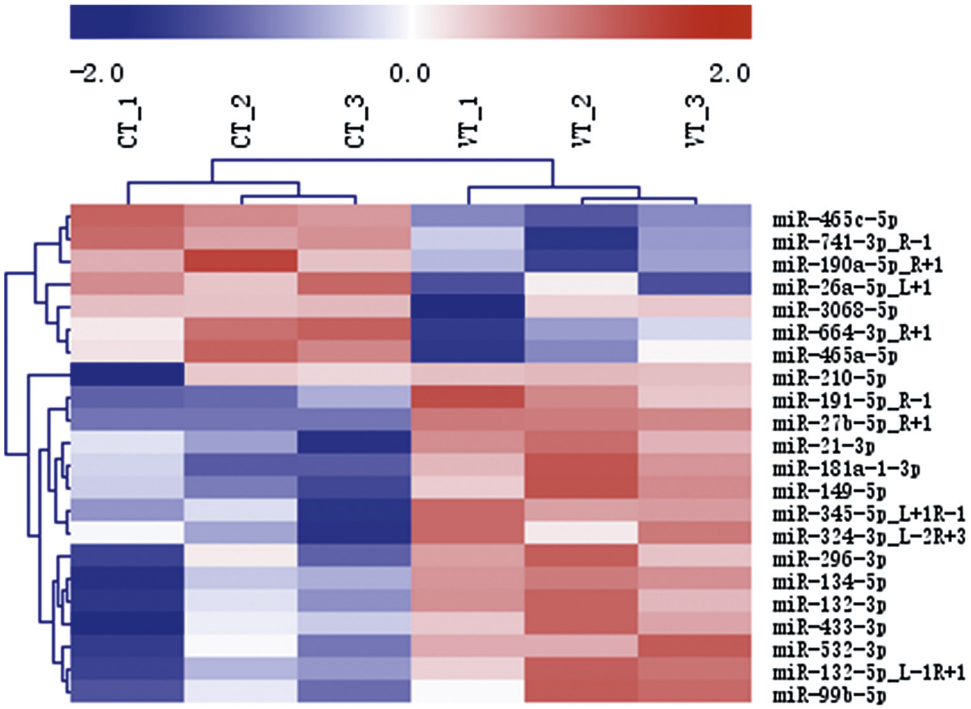

Fig. 2. Unsupervised hierarchical analysis in fresh and vitrified oocytes. Each row represents an individual miRNA while each column represents a biological replicate. The dendrogram at the left and top side display similarity expression among miRNAs and replicates, respectively. CT, fresh oocytes; VT, vitrified oocytes.

was mainly in the range of 21–24 nt. Our results showed that 22 miRNAs were differentially expressed in vitrified oocytes, indicating the regulatory role of miRNAs in response to vitrification. Heat-map analysis demonstrated good reproducibility of oocytes in control and vitrified group as well as among biological technical repeats. And RT-qPCR results further verified the accuracy of sequencing data. To our knowledge, this is the first study elucidating the dynamic changes of miRNAs expression during oocyte vitrification.

Ultrastructural dysmorphisms, including increased vacuolization, aberrant dynamic variations in mitochondria-smooth endoplasmic reticulum and mitochondria-vesicle complexes as well as scarce cortical granules were observed in cryopreserved oocytes (Nottola et al., 2016). Moreover, disturbed mitochondrial localization was found in vitrified mouse oocytes (Yan et al., 2010). Additionally, vitrification would induce damages on microtubules, actin filaments and chromosome integrity in oocytes (Wen et al., 2014). These results were in agreement with our GO enrichment results where the potential targets for the differentially expressed miRNAs were preferentially clustered in “anatomical structure development” in biological process, and “cell” in cellular components, implying that the peculiar structure in oocytes was one of the main obstacles for successful preservation. Pathway enrichment analysis identified significantly enriched endometrial cancer pathway and most assigned metabolic pathway, suggesting vitrification may have an impact on oocytes’ viability and metabolic

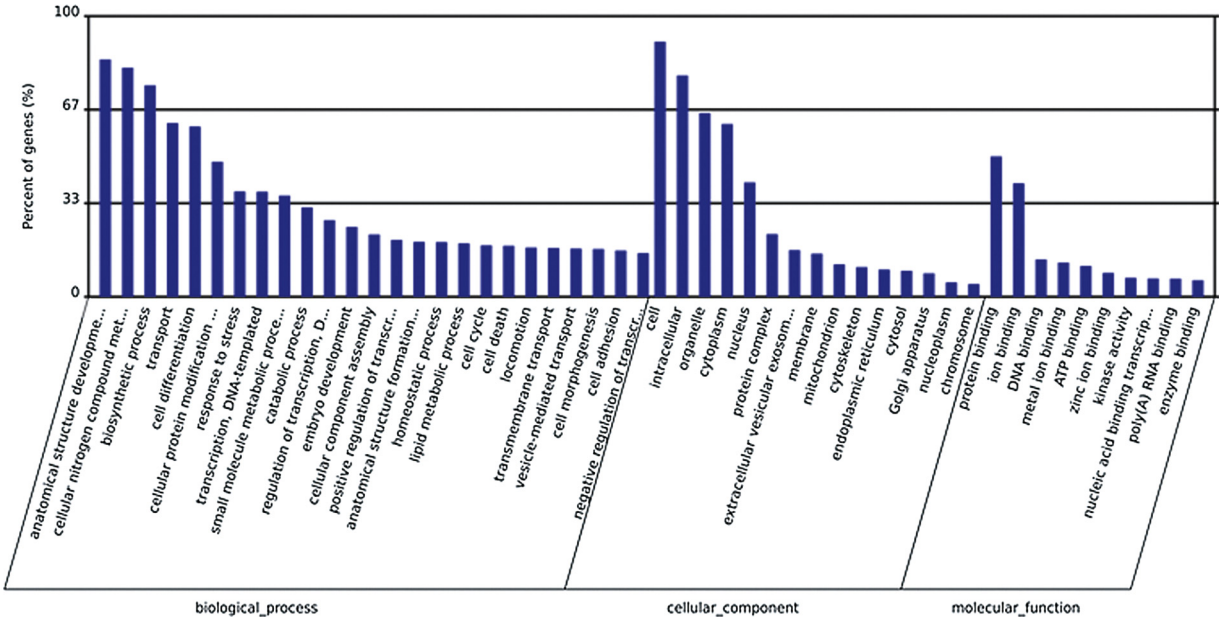

Fig. 3. GO analysis of genes potentially targeted by differentially expressed miRNAs. The vertical axis shows the percentage of genes clustered in each GO term.

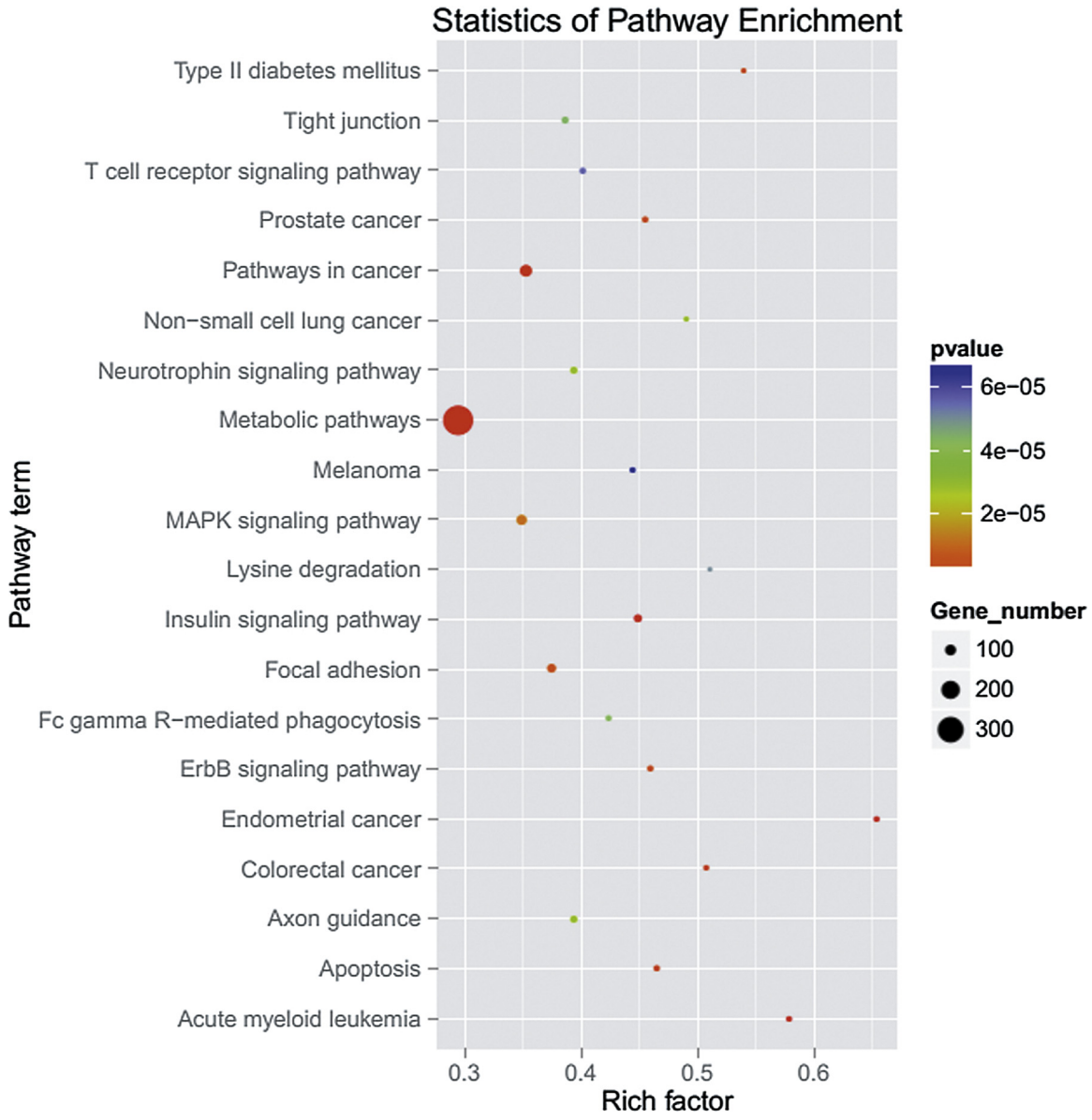

Fig. 4. Scatter plot of KEGG pathway analysis of genes targeted by differentially expressed miRNAs with the top 20 enrichment scores. Rich Factor refers to the ratio generated from dividing gene numbers in a special pathway by the total number of genes. Greater Rich Factor means greater intensiveness.

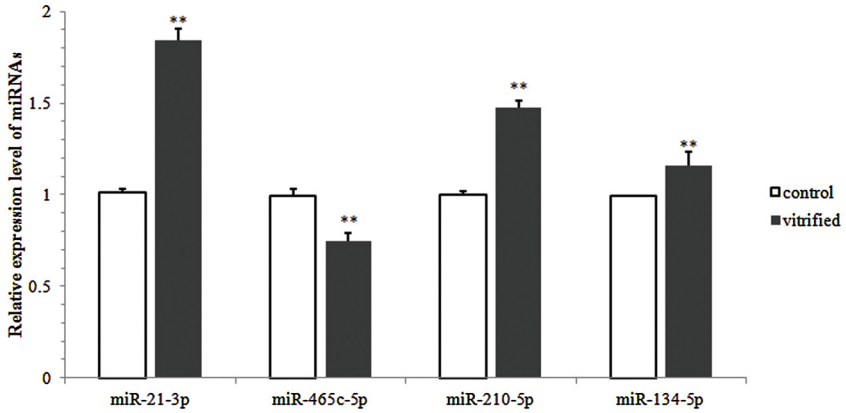

Fig. 5. RT-qPCR validation of RNA sequencing data. RT-qPCR analysis of four individual miRNAs (miR-21-3p, miR-465c-5p, miR-210-5p, and miR-134-5p) in control and vitrified oocytes. Data are presented as means ± SD. **, $P < 0.01$.

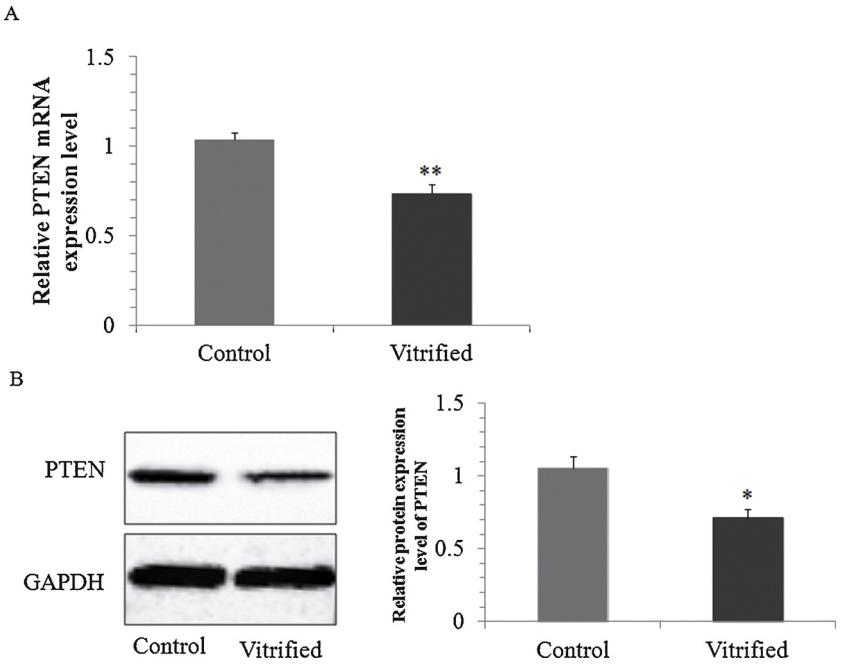

Fig. 6. Changes of PTEN expression after oocyte vitrification. A. Relative mRNA expression level of *PTEN* in fresh and frozen oocytes. B. Protein expression level of PTEN in fresh and vitrified counterparts. Values are expressed as mean ± SD. **, $P < 0.01$.

profile.

During miRNA biogenesis, primary miRNAs were cleaved into miRNA duplexes composed of a guide and a passenger strand (also known as miRNA and miRNA*) (Guo and Lu, 2010). Recent studies showed that many miRNA* species were relatively rich and played important roles in various processes (Jin et al., 2011; Byrd et al., 2012). Our result showed that the expression of miR-21-3p, also known as miR-21*, was increased after vitrification. Target genes of miR-21-3p were identified to be involved in physiological and pathological processes (Yan et al., 2015; Baez-Vega et al., 2016; Xia et al., 2018). It was referred that miR-21-3p could repress the expression of PTEN in umbilical cord blood plasma exosomes (Hu et al., 2018). We also proved that miR-21-3p could down-regulate the expression of PTEN by targeting its 3′UTR. PTEN always functions towards PI3K/AKT pathway, an important signaling in regulating cell apoptosis through the regulation of oxidative stress (Matsuda et al., 2018). Previous study indicated that reduced PTEN expression was associated with elevated reactive oxygen species level (Goo et al., 2012; Li et al., 2013; Noh et al., 2016), which was considered to be accounted for the decreased developmental potential of vitrified oocytes (Pan et al., 2018; Wang et al., 2018a). In addition, it was suggested that repressed PTEN may accumulate DNA damage and negatively affect the quality of oocytes

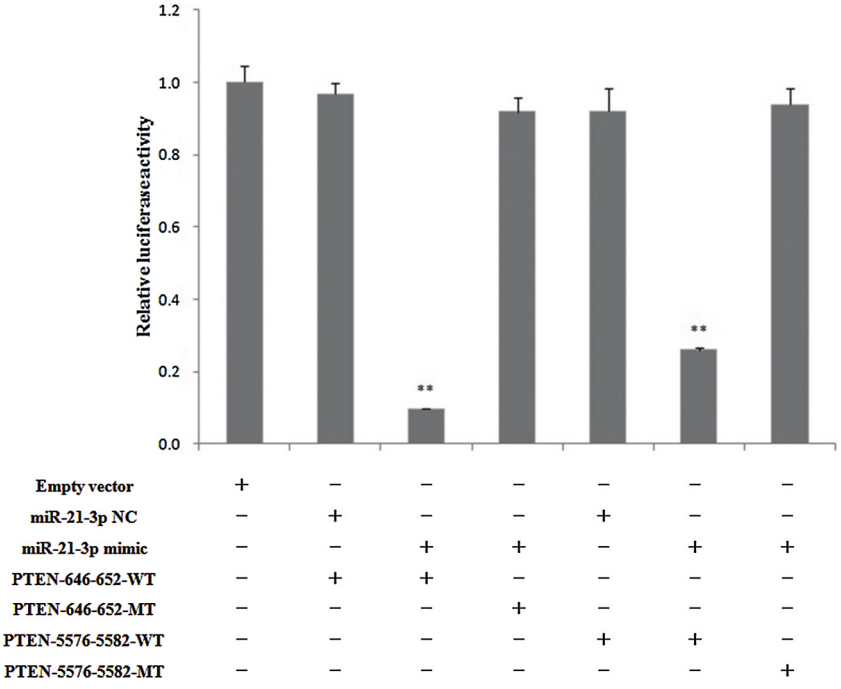

Fig. 7. Identification of the target gene for miR-21-3p. “PTEN-646-652” and “PTEN-5576-5582” represent two binding sites for miR-21-3p in the 3′UTR of PTEN. Results are expressed as mean ± SD. **, $P < 0.01$.

(Maidarti et al., 2019). Thus, it seemed that decreased PTEN expression was related to the limited developmental potential of warmed oocytes.

In conclusion, our results demonstrated that vitrification would induce dynamic changes of miRNAs expression in oocytes, and decreased expression of PTEN mediated by miR-21-3p may associate with the compromised developmental potential of vitrified oocytes.

Funding

This work was supported by the grant from Natural Science Foundation of Hebei province of China [No. H2015206453].

References

Ambros, V., 2004. The functions of animal microRNAs. Nature 431 (7006), 350–355.
Baez-Vega, P.M., Echevarria Vargas, I.M., Valiyeva, F., Encarnacion-Rosado, J., Roman, A., Flores, J., Marcos-Martinez, M.J., Vivas-Mejia, P.E., 2016. Targeting miR-21-3p inhibits proliferation and invasion of ovarian cancer cells. Oncotarget 7 (24), 36321–36337.
Bartel, D.P., 2004. MicroRNAs: genomics, biogenesis, mechanism, and function. Cell 116 (2), 281–297.
Braga, D.P., Setti, A.S., Figueira, R.C., Azevedo Mde, C., Iaconelli Jr., A., Lo Turco, E.G., Borges Jr, E., 2016. Freeze-all, oocyte vitrification, or fresh embryo transfer? Lessons from an egg-sharing donation program. Fertil. Steril. 106 (3), 615–622.
Byrd, A.E., Aragon, I.V., Brewer, J.W., 2012. MicroRNA-30c-2* limits expression of proadaptive factor XBP1 in the unfolded protein response. J. Cell Biol. 196 (6), 689–698.
Capra, E., Turri, F., Lazzari, B., Cremonesi, P., Gliozzi, T.M., Fojadelli, I., Stella, A., Pizzi, F., 2017. Small RNA sequencing of cryopreserved semen from single bull revealed altered miRNAs and piRNAs expression between High- and Low-motile sperm populations. BMC Genomics 18 (1), 14.
Cil, A.P., Seli, E., 2013. Current trends and progress in clinical applications of oocyte cryopreservation. Curr. Opin. Obstet. Gynecol. 25 (3), 247–254.
Gao, L., Jia, G., Li, A., Ma, H., Huang, Z., Zhu, S., Hou, Y., Fu, X., 2017. RNA-Seq transcriptome profiling of mouse oocytes after in vitro maturation and/or vitrification. Sci. Rep. 7 (1), 13245.
Goldman, K.N., Noyes, N.L., Knopman, J.M., McCaffrey, C., Grifo, J.A., 2013. Oocyte efficiency: does live birth rate differ when analyzing cryopreserved and fresh oocytes on a per-oocyte basis? Fertil. Steril. 100 (3), 712–717.
Goo, C.K., Lim, H.Y., Ho, Q.S., Too, H.P., Clement, M.V., Wong, K.P., 2012. PTEN/Akt signaling controls mitochondrial respiratory capacity through 4E-BP1. PLoS One 7 (9), e45806.
Guo, L., Lu, Z., 2010. The fate of miRNA* strand through evolutionary analysis: implication for degradation as merely carrier strand or potential regulatory molecule? PLoS One 5 (6), e11387.
Hu, Y., Rao, S.S., Wang, Z.X., Cao, J., Tan, Y.J., Luo, J., Li, H.M., Zhang, W.S., Chen, C.Y., Xie, H., 2018. Exosomes from human umbilical cord blood accelerate cutaneous wound healing through miR-21-3p-mediated promotion of angiogenesis and fibroblast function. Theranostics 8 (1), 169–184.
Jin, L., Hu, W.L., Jiang, C.C., Wang, J.X., Han, C.C., Chu, P., Zhang, L.J., Thorne, R.F., Wilmott, J., Scolyer, R.A., Hersey, P., Zhang, X.D., Wu, M., 2011. MicroRNA-149*, a p53-responsive microRNA, functions as an oncogenic regulator in human melanoma. Proc Natl Acad Sci U S A 108 (38), 15840–15845.
Karakaya, C., Guzeloglu-Kayisli, O., Uyar, A., Kallen, A.N., Babayev, E., Bozkurt, N., Unsal, E., Karabacak, O., Seli, E., 2015. Poor ovarian response in women undergoing in vitro fertilization is associated with altered microRNA expression in cumulus cells. Fertil. Steril. 103 (6), 1469–1476 e1461-1463.
Li, Y., He, L., Zeng, N., Sahu, D., Cadenas, E., Shearn, C., Li, W., Stiles, B.L., 2013. Phosphatase and tensin homolog deleted on chromosome 10 (PTEN) signaling regulates mitochondrial biogenesis and respiration via estrogen-related receptor alpha (ERRalpha). J. Biol. Chem. 288 (35), 25007–25024.
Lim, L.P., Lau, N.C., Garrett-Engele, P., Grimson, A., Schelter, J.M., Castle, J., Bartel, D.P., Linsley, P.S., Johnson, J.M., 2005. Microarray analysis shows that some microRNAs downregulate large numbers of target mRNAs. Nature 433 (7027), 769–773.
Maidarti, M., Clarkson, Y.L., McLaughlin, M., Anderson, R.A., Telfer, E.E., 2019. Inhibition of PTEN activates bovine non-growing follicles in vitro but increases DNA damage and reduces DNA repair response. Hum. Reprod. 34 (2), 297–307.
Matsuda, S., Nakagawa, Y., Kitagishi, Y., Nakanishi, A., Murai, T., 2018. Reactive oxygen species, superoxide dimutases, and PTEN-p53-AKT-MDM2 signaling loop network in mesenchymal stem/stromal cells regulation. Cells 7 (5).
Noh, E.M., Park, J., Song, H.R., Kim, J.M., Lee, M., Song, H.K., Hong, O.Y., Whang, P.H., Han, M.K., Kwon, K.B., Kim, J.S., Lee, Y.R., 2016. Skin aging-dependent activation of the PI3K signaling pathway via downregulation of PTEN increases intracellular ROS in human dermal fibroblasts. Oxid. Med. Cell. Longev. 2016, 6354261.
Nottola, S.A., Albani, E., Coticchio, G., Palmerini, M.G., Lorenzo, C., Scaravelli, G., Borini, A., Levi-Setti, P.E., Macchiarelli, G., 2016. Freeze/thaw stress induces organelle remodeling and membrane recycling in cryopreserved human mature oocytes. J. Assist. Reprod. Genet. 33 (12), 1559–1570.
Pan, B., Yang, H., Wu, Z., Qazi, I.H., Liu, G., Han, H., Meng, Q., Zhou, G., 2018. Melatonin improves parthenogenetic development of vitrified(-)warmed mouse oocytes potentially by promoting G1/S cell cycle progression. Int. J. Mol. Sci. 19 (12).
Practice Committees of American Society for Reproductive, M, Society for Assisted Reproductive, T, 2013. Mature oocyte cryopreservation: a guideline. Fertil. Steril. 99 (1), 37–43.
Rienzi, L., Gracia, C., Maggiulli, R., LaBarbera, A.R., Kaser, D.J., Ubaldi, F.M., Vanderpoel, S., Racowsky, C., 2017. Oocyte, embryo and blastocyst cryopreservation in ART: systematic review and meta-analysis comparing slow-freezing versus vitrification to produce evidence for the development of global guidance. Hum. Reprod. Update 23 (2), 139–155.
Song, C., Yao, J., Cao, C., Liang, X., Huang, J., Han, Z., Zhang, Y., Qin, G., Tao, C., Li, C., Yang, H., Zhao, J., Li, K., Wang, Y., 2016. PPARgamma is regulated by miR-27b-3p negatively and plays an important role in porcine oocyte maturation. Biochem. Biophys. Res. Commun. 479 (2), 224–230.
Succu, S., Gadau, S.D., Serra, E., Zinellu, A., Carru, C., Porcu, C., Naitana, S., Berlinguer, F., Leoni, G.G., 2018. A recovery time after warming restores mitochondrial function and improves developmental competence of vitrified ovine oocytes. Theriogenology 110, 18–26.
Tscherner, A., Brown, A.C., Stalker, L., Kao, J., Dufort, I., Sirard, M.A., LaMarre, J., 2018. STAT3 signaling stimulates miR-21 expression in bovine cumulus cells during in vitro oocyte maturation. Sci. Rep. 8 (1), 11527.
Wang, T.Y., Zhang, J., Zhu, J., Lian, H.Y., Yuan, H.J., Gao, M., Luo, M.J., Tan, J.H., 2017. Expression profiles and function analysis of microRNAs in postovulatory aging mouse oocytes. Aging (Albany NY) 9 (4), 1186–1201.
Wang, Y., Zhang, M., Chen, Z.J., Du, Y., 2018a. Resveratrol promotes the embryonic development of vitrified mouse oocytes after in vitro fertilization. In Vitro Cell. Dev. Biol. Anim. 54 (6), 430–438.
Wang, Y., Zhang, M.L., Zhao, L.W., Kuang, Y.P., Xue, S.G., 2018b. Enhancement of the efficiency of oocyte vitrification through regulation of histone deacetylase 6 expression. J. Assist. Reprod. Genet. 35 (7), 1179–1185.
Wen, Y., Zhao, S., Chao, L., Yu, H., Song, C., Shen, Y., Chen, H., Deng, X., 2014. The protective role of antifreeze protein 3 on the structure and function of mature mouse oocytes in vitrification. Cryobiology 69 (3), 394–401.
Xia, B., Lu, J., Wang, R., Yang, Z., Zhou, X., Huang, P., 2018. miR-21-3p regulates influenza a virus replication by targeting histone Deacetylase-8. Front. Cell. Infect. Microbiol. 8, 175.
Yan, C.L., Fu, X.W., Zhou, G.B., Zhao, X.M., Suo, L., Zhu, S.E., 2010. Mitochondrial behaviors in the vitrified mouse oocyte and its parthenogenetic embryo: effect of Taxol pretreatment and relationship to competence. Fertil. Steril. 93 (3), 959–966.
Yan, M., Chen, C., Gong, W., Yin, Z., Zhou, L., Chaugai, S., Wang, D.W., 2015. miR-21-3p regulates cardiac hypertrophic response by targeting histone deacetylase-8. Cardiovasc. Res. 105 (3), 340–352.
Zhao, X., Hao, H., Du, W., Zhu, H., 2015. Effect of vitrification on the microRNA transcriptome in mouse blastocysts. PLoS One 10 (4), e0123451.